Proceedings of the IEEE ITSC 2006
2006 IEEE Intelligent Transportation Systems Conference
Toronto, Canada, September 17-20, 2006

Trajectory Planning with Velocity Planner for Fully-automated Passenger Vehicles

Razvan Solea and Urbano Nunes, *Member, IEEE*

***Abstract*— For fully-automated passenger vehicles, trajectory planning that produce smooth trajectories, with respect to the comfort of human body, is required. An approach that consists of introducing a velocity planning stage to generate adequate time sequences to be used in the interpolating curve planner, is proposed. The generated speed profile can be merged into the trajectory for usage in trajectory-tracking tasks or it can be used for path-following tasks. Moreover, this paper presents design and simulation evaluation of trajectory-tracking and path-following controllers for autonomous vehicles based on sliding mode control.**

I. INTRODUCTION

Fully-automated passenger vehicles are expected to be widely used in urban areas, airport terminals, pedestrian zones, etc [1], [2] and [3]. Although motion planning of mobile robots and autonomous vehicles has been thoroughly studied in the last decades, the requisite of producing trajectories with low associated accelerations and jerk is not easily traceable in the technical literature. This paper addresses this problem proposing an approach that consists of introducing a velocity planning stage to generate adequate time sequences to be used in the interpolating curve planners. In this context, we generate speed profiles (linear and angular) that lead to respecting human comfort travel. The need of having travel comfort in autonomous vehicle' applications, like in cybercars [2], motivated our research on the subject of this paper. Additionally, control strategies are here proposed using sliding mode control (SMC) techniques. In order to model a realistic trajectory tracking problem, the car is supposed to move forward only.

Human sensation of the ride comfort (or ride discomfort) is a psycho-physical process of responding to physical stimuli. To understand human judgment of ride comfort, seeking the physical stimuli is of great importance [4]. Physical dynamic quantities (motion quantities) are usually: acceleration (lateral, longitudinal and vertical) and angular motions (roll, pitch and yaw). Some of these quantities are evaluated by international standards or by company standards. Types of comfort disturbances can be grouped in: (i) direct comfort disturbance caused by a sudden motion of the vehicle, resulting in discomfort; (ii) the second type of disturbance is caused by high lateral accelerations and/or lateral jerks while negotianting transition curve. These accelerations and jerks are results of a changing track geometry [5].

The trajectory tracking control, which is one of the three basic navigation problems [6], means tracking reference trajectories predefined or given by path planners. In the last ten years, there are so ample research works on the trajectory tracking control of vehicles that various effective methods and tracking controllers have been developed. The model-based tracking and following approaches can be divided into kinematic and dynamic based methods.

According to different control theories, a more elaborate category in the sense of kinematic methods can be grouped in five sets [7]: (1) sliding mode based approaches, (2) input-output linearization based approaches, (3) fuzzy based approaches, (4) neural network based approaches, and (5) back-stepping based approaches. Among all of these kinematic-based methods, considering the stability of tracking control laws, the hardware computation load and the maneuverability in practice, tracking control law designed by sliding mode technology has been proved one of the best solutions.

Sliding mode control is a special discontinuous control technique applicable to various systems [8]. By designing switch functions of state variables or output variables to form sliding surfaces, SMC can guarantee that when trajectories reach the surfaces, the switch functions keep the trajectories on the surfaces, thus yielding the desired system dynamics. The main advantages of using SMC include fast response, good transient and the robustness with respect to system uncertainties and external disturbances. Therefore, it is attractive for many highly nonlinear uncertain systems [9].

This paper is organized as follows. Section II describes the trajectory planning of the vehicle. In section III, trajectory-tracking and path-following error models are presented for simple vehicle model (bicycle model). In sections IV and V sliding mode controllers are proposed for this model. Some simulation results are presented in section VI. Conclusions are presented in section VII.

II. TRAJECTORY PLANNING

Trajectory planning for passenger's transport vehicles must generate smooth trajectories with low associated accelerations and jerk. Lateral and longitudinal accelerations depend on the linear speed:

$$a_T = \frac{dv}{dt}, \tag{1}$$

$$a_L = \frac{d\theta}{dt} \cdot v = k \cdot v^2, \tag{2}$$

This work was supported in part by FCT (Portuguese Foundation for Science and Technology) under Grant: POSC/EEA-SRI/58016/2004, and project CyberC3 (European Asia ITC Programme). Razvan Solea benefited a research fellowship from FCT: SFRH/BD/18244/2004.

R. Solea is with the Institute of Systems and Robotics, University of Coimbra, 3030 Portugal (phone: 351-239-796200, fax: 351-239-406672), razvan@isr.uc.pt

U. Nunes is with the Institute of Systems and Robotics, University of Coimbra, 3030 Portugal, urbano@deec.uc.pt

1-4244-0094-5/06/$20.00 ©2006 IEEE

thus, the trajectory planning must perform not only the planning of the curve (spatial dimension) but also the speed profile (temporal dimension).

From (2) we observe that the lateral acceleration is function of the trajectory curvature (k) and speed (v). For constant speed, the smaller is the curvature the smaller is the induced lateral acceleration, and therefore less harmful effects on the passenger.

The ISO 2631-1 standard [10] (Table 1) relates comfort with the overall r.m.s. acceleration, acting on the human body, defined as:

$$a_w = \sqrt{k_x^2 \cdot a_{wx}^2 + k_y^2 \cdot a_{wy}^2 + k_z^2 \cdot a_{wz}^2} \tag{3}$$

where a_{wx}, a_{wy}, a_{wz}, are the r.m.s. accelerations on x, y, z axes respectively, and k_x, k_y, k_z, are multiplying factors. For a seated person $k_x = k_y = 1.4$, $k_z = 1$. For motion on the $x-y$ plane, $a_{wz} = 0$. The local coordinate system is chosen so that the x-axis is the longitudinal trajectory direction, and y-axis is the lateral trajectory direction.

TABLE I
ISO 2631-1 STANDARD.

Overall Acceleration	Consequence
$a_w < 0.315 m/s^2$	Not uncomfortable
$0.315 < a_w < 0.63 m/s^2$	A little uncomfortable
$0.5 < a_w < 1 m/s^2$	Fairy uncomfortable
$0.8 < a_w < 1.6 m/s^2$	Uncomfortable
$1.25 < a_w < 2.5 m/s^2$	Very uncomfortable
$a_w > 2.5 m/s^2$	Extremely uncomfortable

Using Table I and equation (3), for "not uncomfortable" accelerations, the longitudinal and lateral r.m.s. accelerations must be less than 0.21 m/s^2. This value allows defining the reference speeds, and consequently the time values.

The reference velocity at the final point of a segment k (defined by two consecutive waypoints i and $i+1$), can be calculated as

$$v_{i+1} = v_i \pm a_{wx} \cdot t_k, \; a_{wx} \leq 0.21 m/s^2 \tag{4}$$

$$t_k = t_{i+1} - t_i = \sqrt{\frac{2 \cdot s_k}{a_{wx}}} \tag{5}$$

where s_k is the length of the segment.

A path between the initial and the final point is formed as a series of segments (each segment connects two consecutive waypoints).

The problem: Given a set of points, find control inputs $v(t)$, $\omega(t)$ such that the car-like vehicle starting from an arbitrary initial extended state:
$p_a = [x_a \; y_a]^T = [x(0) \; y(0)]^T$; $\theta_a = \theta(0)$;
$v_a = v(0); \dot{v}_a = \dot{v}(0); \omega_a = \omega(0); \dot{\omega}_a = \dot{\omega}(0)$
reaches the arbitrary final extended state:
$p_w = [x_w \; y_w]^T = [x(t_{fin}) \; y(t_{fin})]^T$; $\theta_w = \theta(t_{fin})$;
$v_w = v(t_{fin}); \dot{v}_w = \dot{v}(t_{fin}); \omega_w = \omega(t_{fin}); \dot{\omega}_w = \dot{\omega}(t_{fin})$
crossing all the given points. The comfort of human body constraint

$$a_w < 0.4 m/s^2 \tag{6}$$

TABLE II
TRAJECTORY PLANNING ALGORITHM.

1. calculate $x_k(u)$ and $y_k(u)$ for each curve (eq. 8).
2. calculate the curve length s_k for each curve (eq. 7).
3. calculate the curvature for each curve:
   $k_{ck}(u) = \frac{\dot{x}_k(u) \cdot \ddot{y}_k(u) - \ddot{x}_k(u) \cdot \dot{y}_k(u)}{\sqrt{\dot{x}_k^2(u) + \dot{y}_k^2(u)}}$
4. calculate the time t_k for each curve (eq. 5).
5. calculate velocity at each waypoint v_i (eq. 4).
6. repeat (for each curve)
   (a) calculate the curvature, $k_k(s_k)$
   (b) calculate $v_k(t)$
   (b1) if $min(v_k(t)) < 0$ then decrease the final velocity v_{i+1} and go to (b).
   (c) calculate the angular velocity $\omega_k(t)$ (eq. 10).
   (d) find the overall rms acceleration a_{wk} (eq. 3).
   (e) if $a_{wk} > 0.4 m/s^2$ then increase the time (t_k).
7. until $a_{wk} < 0.4 m/s^2$.

is to be satisfied.

• Step 1: Determine a path connecting p_a (start point) with p_w (final point), and calculate the length s for each curve:

$$s_k = \int_0^1 \|\dot{p}_k(\xi)\| \cdot d\xi \tag{7}$$

This corresponds to find a set of curves

$$p_k(u) = \begin{bmatrix} x_k(u) \\ y_k(u) \end{bmatrix} = \\ = \begin{bmatrix} c_{0k} + c_{1k} \cdot u + c_{2k} \cdot u^2 + \dots \\ d_{0k} + d_{1k} \cdot u + d_{2k} \cdot u^2 + \dots \end{bmatrix} \tag{8}$$

were $u \in [0, \; 1]$, and c_{ik} and d_{ik}, $i = 1, 2, \dots$ are constants to be found function of the type of the curve (e.g. cubic splines, trigonometric splines or quintic splines).

• Step 2: $v_k(t)$ is generated with five properly joined spline curves $(j = 1, 2, \dots 5)$ like in [11]:

$$v_j(t) = a_{1j} + 2a_{2j} \cdot t + 3a_{3j} \cdot t^2 \tag{9}$$

The generated velocity is C^1 and strictly positive for any $t \in (0, t_k)$. The time is calculated for each curve using (5).

• Step 3: The angular velocity functions $\omega_k(t) \in C^1$ are defined according to:

$$\omega_k(t) := v_k(t) \cdot k_k(s_k)\big|_{s_k = \int_0^t v_k(\xi) d\xi} \tag{10}$$

where $k_k(s_k)$ is the curvature expressed as a function of the arc length s_k.

• Step 4: Calculate the r.m.s. acceleration a_{wk} for each curve using equations (1), (2) and (3).

IF $a_{wk} > 0.4 m/s^2$

THEN change the time for that segment (curve) and go to step 2.

If the r.m.s. acceleration is not under $0.4 m/s^2$ for a given curve the time for that segment should be increased. Using the proposed algorithm (summarized in Table II) a path, respecting comfort of human body, is obtained.

Consider the example depicted in Fig. 1 where the larger circles represent waypoints $(a, b, ..., g)$ and smaller circles

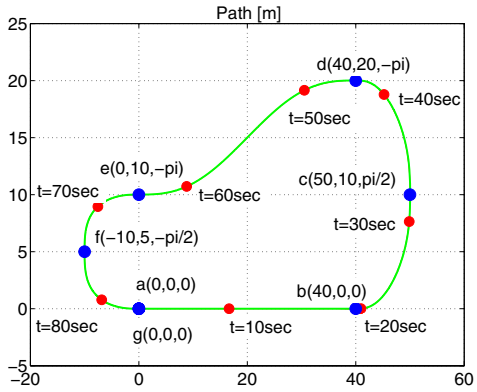

Fig. 1. Path planning example using quintic polynomial curves

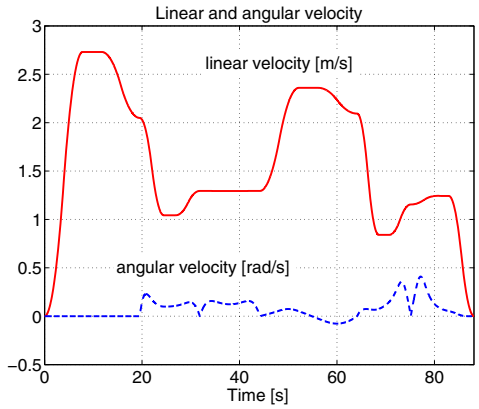

Fig. 2. Linear and angular velocities for path example

represent time values $(10, 20, ..., 80s)$ which are shown to turn more understandable the method for the reader. Each waypoint is defined by a position, in meters, and an orientation, in radians.

Figures 1-3 show results of the application of the proposed trajectory planning algorithm satisfying the comfort condition (6). From Fig. 3 we observe that the maximum absolute value for lateral acceleration is bellow than $0.5m/s^2$ and the maximum absolute value for longitudinal acceleration is bellow $0.7m/s^2$.

Table III summarizes the results of the applied trajectory planning algorithm: length, time and r.m.s. acceleration values for each curve (segment). Three acceleration components are considered: lateral, longitudinal and overall acceleration. In accordance with the 6^{th} column of Table III, a_{wk} satisfies (6), i.e. $a_w < 0.4m/s^2$. This value is between "Not uncomfortable" and "A little uncomfortable" (see Table I).

III. TRAJECTORY-TRACKING AND PATH-FOLLOWING ERROR MODELS

We consider as a motion model of a vehicle the following simplified nonholonomic system:

$$\begin{cases} \dot{x}_r(t) = v_r(t) \cdot cos\theta_r(t) \\ \dot{y}_r(t) = v_r(t) \cdot sin\theta_r(t) \\ \dot{\theta}_r(t) = \frac{v_r}{l} \cdot tan\phi_r(t) \end{cases} \quad (11)$$

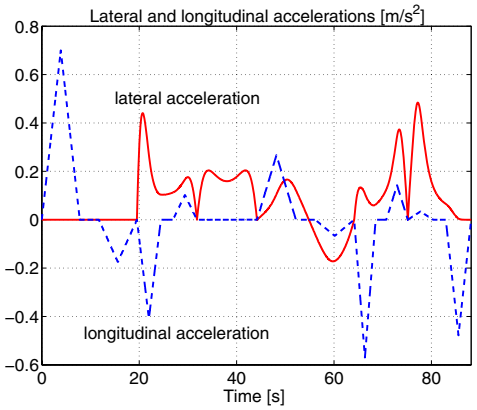

Fig. 3. Lateral and longitudinal accelerations for path example

TABLE III
LENGTH, TIME AND R.M.S. ACCELERATION VALUES FOR EACH CURVE

no	s_k $[m]$	t_k $[s]$	a_{wx_k} $[m/s^2]$	a_{wy_k} $[m/s^2]$	a_{w_k} $[m/s^2]$
1	40.0000	19.5200	0.2633	0.0000	0.3686
2	15.9500	12.3200	0.1537	0.2002	0.3534
3	15.9500	12.3200	0.0001	0.1703	0.2385
4	41.7500	19.9400	0.1005	0.1112	0.2098
5	12.7000	11.0000	0.2143	0.1783	0.3903
6	12.7000	13.0000	0.1749	0.2098	0.3824
	139.0500	88.1000	0.1766	0.1514	0.3257

where (see Fig. 4) x_r and y_r are the Cartesian coordinates of the rear axle midpoint, v_r is the velocity of this midpoint, θ_r is the vehicle's heading angle, l is the inter-axle distance, and ϕ_r the front wheel angle, which is the control variable to steer the vehicle.

In this paper, the kinematic bicycle model is considered (see Figs. 5 and 6). The trajectory tracking errors can be described by (x_e, y_e, θ_e). The aim is to design a stable controller with commands (v_c, ϕ_c).

The error vector for trajectory-tracking is easily obtained from Fig. 4 and 5,

$$\begin{bmatrix} x_e \\ y_e \\ \theta_e \end{bmatrix} = \begin{bmatrix} cos\theta_d & sin\theta_d & 0 \\ -sin\theta_d & cos\theta_d & 0 \\ 0 & 0 & 1 \end{bmatrix} \cdot \begin{bmatrix} x_r - x_d \\ y_r - y_d \\ \theta_r - \theta_d \end{bmatrix} \quad (12)$$

where (x_d, y_d, θ_d) denotes the virtual car pose. The corre-

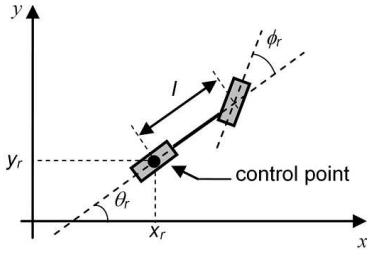

Fig. 4. Bicycle model (11)

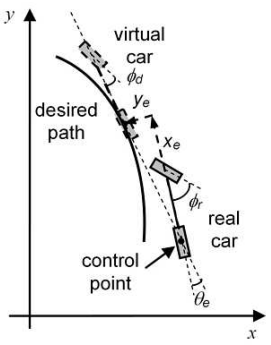

Fig. 5. Lateral, longitudinal and orientation error (trajectory-tracking)

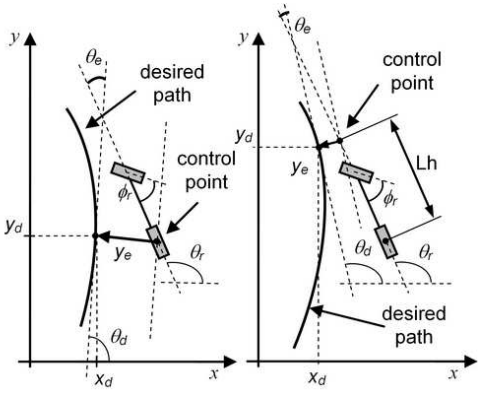

Fig. 6. Lateral and orientation errors for path-following without and with look-ahead distance (Lh)

sponding error derivatives are

$$\begin{cases} \dot{x}_e = -v_d + v_r \cdot cos\theta_e + y_e \cdot \frac{v_d}{l} \cdot tan\phi_d \\ \dot{y}_e = v_r \cdot sin\theta_e - x_e \cdot \frac{v_d}{l} \cdot tan\phi_d \\ \dot{\theta}_e = \frac{v_r}{l} \cdot tan\phi_r - \frac{v_d}{l} \cdot tan\phi_d \end{cases} \tag{13}$$

where v_d and ϕ_d are the heading speed and desired front wheel angle, respectively.

For the path-following without Look-ahead ($Lh = 0$) (see Fig. 6) the error vector is:

$$\begin{bmatrix} y_e \\ \theta_e \end{bmatrix} = T \cdot \begin{bmatrix} x_r - x_d \\ y_r - y_d \\ \theta_r - \theta_d \end{bmatrix} \tag{14}$$

where $T = \begin{bmatrix} -sin\theta_d & cos\theta_d & 0 \\ 0 & 0 & 1 \end{bmatrix}$.

The lateral error, y_e, is defined as the distance between the vehicle control point (CP) and the closest point along the desired trajectory. The corresponding error derivatives are:

$$\begin{cases} \dot{y}_e = v_r \cdot sin\theta_e \\ \dot{\theta}_e = \dot{\theta}_r = \frac{v_r}{l} \cdot tan\phi_r \end{cases} \tag{15}$$

Defining the control point CP (see Fig. 6) at a distance $Lh \neq 0$ in front of the robot (called Look-ahead distance), (14) becomes:

$$\begin{bmatrix} y_e \\ \theta_e \end{bmatrix} = T \cdot \begin{bmatrix} x_r - x_d + Lh \cdot cos\theta_r \\ y_r - y_d + Lh \cdot sin\theta_r \\ \theta_r - \theta_d \end{bmatrix}$$

and

$$\begin{cases} \dot{y}_e = v_r \cdot sin\theta_e + Lh \cdot \frac{v_r}{l} \cdot tan\phi_r \cdot cos\theta_e \\ \dot{\theta}_e = \dot{\theta}_r = \frac{v_r}{l} \cdot tan\phi_r \end{cases} \tag{16}$$

In this paper it is assumed that $|\theta_e| < \pi/2$, which means that the vehicle orientation must not be perpendicular to the desired trajectory.

IV. SLIDING-MODE TRAJECTORY-TRACKING CONTROL

It is supposed that a feasible desired trajectory for the car-like vehicle is pre-specified by a trajectory planner. The problem is to design a robust controller so that the vehicle will correctly track the desired trajectory under a large class of disturbances.

A new design of sliding surface is proposed, such that lateral error, y_e, and angular error, θ_e, are internally coupled with each other in a sliding surface leading to convergence of both variables. For that purpose the following sliding surfaces are proposed:

$$s_1 = \dot{x}_e + k_1 \cdot x_e \tag{17}$$

$$s_2 = \dot{y}_e + k_2 \cdot y_e + k_0 \cdot sgn(y_e) \cdot \theta_e \tag{18}$$

A practical general form of reaching the control law is defined as

$$\dot{s} = -Q \cdot s - P \cdot sgn(s) \tag{19}$$

where Q and P are constant positive values. By adding the proportional rate term $-Q \cdot s$, the state is forced to approach the switching manifold faster when s is large.

From the time derivations of (17) and (18), and knowing that

$$\dot{\theta}_e = \dot{\theta}_r - \dot{\theta}_d = \omega_r - \omega_d = \frac{v_r}{l} \cdot tan(\phi_r) - \omega_d$$

after some mathematical manipulation, one can achieve

$$\dot{v}_c = \frac{1}{cos\theta_e} \cdot (-Q_1 \cdot s_1 - P_1 \cdot sgn(s_1) - k_1 \cdot \dot{x}_e - \\ -\dot{\omega}_d \cdot y_e - \omega_d \cdot \dot{y}_e + v_r \cdot \dot{\theta}_e \cdot sin\theta_e + \dot{v}_d) \tag{20}$$

$$\phi_c = arctan(\frac{l}{v_r} \cdot \omega_d + \frac{l}{v_r \cdot (v_r \cdot cos\theta_e + k_0 \cdot sgn(y_e))} \cdot (-Q_2 s_2 - \\ -P_2 sgn(s_2) - k_2 \cdot \dot{y}_e - \dot{v}_r \cdot sin\theta_e + \dot{\omega}_d \cdot x_e + \omega_d \cdot \dot{x_e})) \tag{21}$$

Let us define $V = \frac{1}{2} \cdot s^T \cdot s$ as a Lyapunov function candidate, therefore its time derivative is

$$\begin{aligned} \dot{V} &= s_1 \cdot \dot{s}_1 + s_2 \cdot \dot{s}_2 \\ &= s_1 \cdot (-Q_1 \cdot s_1 - P_1 \cdot sgn(s_1)) + \\ &\quad + s_2 \cdot (-Q_2 \cdot s_2 - P_2 \cdot sgn(s_2)) \\ &= -s^T \cdot Q \cdot s - P_1 \cdot |s_1| - P_2 \cdot |s_2| \end{aligned}$$

For $\dot{V}$ to be negative semi-definite, it is sufficient to choose Q_i and P_i such that $Q_i, P_i \geq 0$.

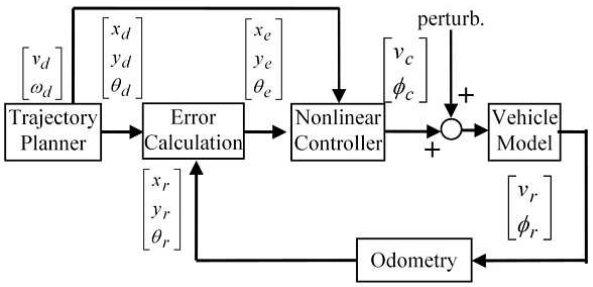

Fig. 7. Simulation model block diagram

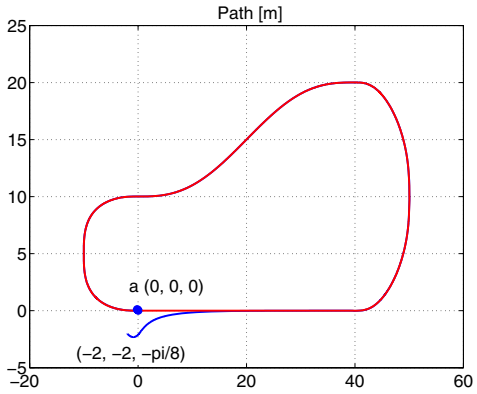

Fig. 8. $x-y$ plot of the car-like vehicle path (desired and followed) with initial pose error: $x_0 = -2, y_0 = -2, \theta_0 = -\pi/8$; a is initial point of the desired trajectory

V. SLIDING-MODE PATH-FOLLOWING CONTROL

The control objective is to ensure that the vehicle will correctly follow the reference path. For this purpose, both the lateral error, y_e, and the orientation error, θ_e, must be minimized. It is supposed that a feasible desired path for the car-like vehicle is pre-specified by a trajectory planner. We propose a new design of sliding surface such that lateral error, y_e, and angular variable, θ_e are internally coupled with each other in a sliding surface leading to convergence of both variables. For that purpose the following sliding surface is proposed:

$$s = \dot{y}_e + k \cdot y_e + k_0 \cdot sgn(y_e) \cdot \theta_e \tag{22}$$

whose time derivative is:

$$\dot{s} = v_r \cdot \dot{\theta}_e \cdot cos\theta_e + k \cdot v_r \cdot sin\theta_e + k_0 \cdot sgn(y_e) \cdot \dot{\theta}_e \tag{23}$$

From (19), (23) and knowing that

$$\dot{\theta}_e = \dot{\theta}_r - \dot{\theta}_d = \frac{v_r}{l} \cdot tan(\phi_r)$$

one gets the steering command

$$\phi_c = arctan\left(\frac{l}{v_r} \cdot \frac{-Qs - Psgn(s) - kv_r sin\theta_e}{v_r \cdot cos\theta_e + k_0 \cdot sgn(y_e)}\right) \tag{24}$$

For the case of using look-ahead Lh:

$$\dot{\phi}_c = \frac{l \cdot cos^2(\phi_r)}{v_r \cdot Lh \cdot cos\theta_e} \cdot (-Q \cdot s - P \cdot sgn(s) - k \cdot \dot{y}_e -$$

$$-v_r \cdot \dot{\theta}_e \cdot cos\theta_e + Lh \cdot \dot{\theta}_e^2 \cdot sin\theta_e - k_0 \cdot sgn(y_e) \cdot \dot{\theta}_e) \tag{25}$$

Let us define $V = \frac{1}{2} \cdot s^2$ as a Lyapunov function candidate, therefore its time derivative is

$$\begin{aligned} \dot{V} &= s \cdot \dot{s} \\ &= s \cdot (\ddot{y}_e + k \cdot \dot{y}_e + k_0 \cdot sgn(y_e) \cdot \dot{\theta}_e) \\ &= s \cdot (-Q \cdot s - P \cdot sgn(s)) \\ &= -Q \cdot s^2 - P \cdot \frac{s^2}{|s|} \end{aligned}$$

For $\dot{V}$ to be negative semi-definite, it is sufficient to choose Q and P such that $Q, P \geq 0$.

VI. SIMULATION RESULTS

The simulation model block diagram is shown in Fig. 7.

The following linearized steering actuator model was employed:

$$H_a = \frac{\phi_r}{\phi_c} = \frac{\omega_n^2}{s^2 + 2 \cdot D \cdot \omega_n \cdot s + \omega_n^2} \tag{26}$$

with $D = 0.7$ and $\omega_n = 2\pi \cdot 5Hz$.

The reference trajectory was generated using the trajectory planner, described in section II (we considered example illustrated in Fig. 1). Table IV summarizes results of simulations for the following cases:

- *trajectory-tracking:*
- A. without initial errors ($x_r(0) = 0$, $y_r(0) = 0$, $\theta_r(0) = 0$);
- B. $x_r(0) = -2$, $y_r(0) = -2$, $\theta_r(0) = -\pi/8$ - results shown in Figs. 8-12;
- C. with input disturbances (Gaussian random noises with zero mean and variance 0.05);
- *path-following*:
- D. without initial errors - results shown in Figs. 13-15;
- E. with input disturbances (Gaussian random noises with zero mean and variance 0.05);
- F. with look ahead distance (Lh), without initial errors.

The overall r.m.s accelerations, for all cases, are under $0.5m/s^2$ ("a little uncomfortable", see Table I). Only in case B (with initial errors) and case E (with perturbations) the lateral r.m.s. acceleration are over $0.21m/s^2$. If we compare all the values of case A with case D, and case C with case E we observe that the trajectory-tracking method gives better results than path-following. Case F (with look-ahead distance) gives better results in comparison with case D (without look-ahead).

Following, two examples, from the complete set of simulations, will be presented. In first example (see Fig. 8) we consider trajectory-tracking method with initial pose error ($x_r(0) = -2$, $y_r(0) = -2$, $\theta_r(0) = -\pi/8$).

Figures 9-12 show longitudinal, lateral and orientation errors and velocities (angular and linear) for the example of

TABLE IV

SIMULATION RESULTS FOR THE TRAJECTORY-TRACKING AND PATH-FOLLOWING CONTROLLER

		A	B	C	D	E	F
Max. Longitudinal Error	$[m]$	0.0522	2.0000	0.0019	-	-	-
r.m.s. Longitudinal Error	$[m]$	0.0166	0.2581	0.0066	-	-	-
Max. Lateral Error	$[m]$	0.0085	2.3125	0.1682	0.0395	0.0279	0.0285
r.m.s. Lateral Error	$[m]$	0.0024	0.4321	0.0542	0.0066	0.0061	0.0062
Max. Angular Error	$[rad]$	0.0083	0.5664	0.0955	0.1195	0.1315	0.1072
r.m.s. Angular Error	$[rad]$	0.0021	0.0831	0.0219	0.0271	0.0303	0.0263
Max. Lateral Acceleration	$[m/s^2]$	0.4889	1.6842	0.6969	0.6292	1.3795	0.4795
r.m.s. Lateral Accelereration	$[m/s^2]$	0.1438	0.2613	0.1839	0.1458	0.2549	0.1391
Max. Longitudinal Acceleration	$[m/s^2]$	0.7493	1.6258	0.7005	0.7002	0.7002	0.7002
r.m.s. Longitudinal Acceleration	$[m/s^2]$	0.1745	0.1946	0.1773	0.1766	0.1766	0.1766
Overal r.m.s. Acceleration	$[m/s^2]$	0.3166	0.4562	0.3577	0.3207	0.4342	0.3148

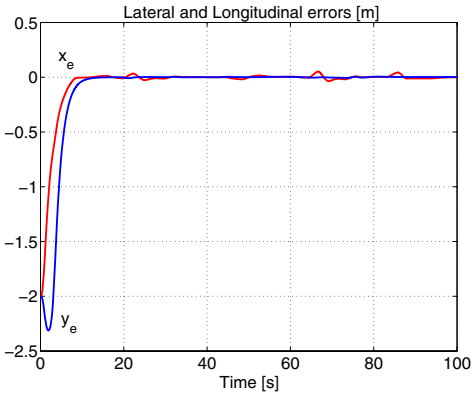

Fig. 9. Lateral (y_e) and longitudinal (x_e) errors

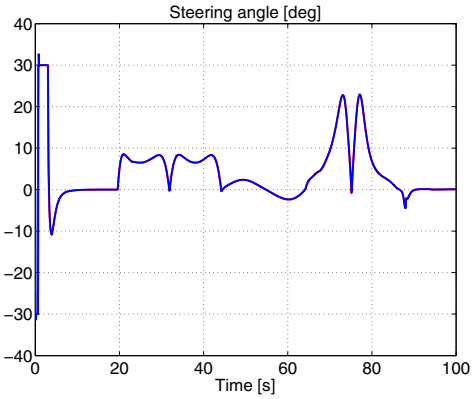

Fig. 11. The steering angle (ϕ_d and ϕ_r)

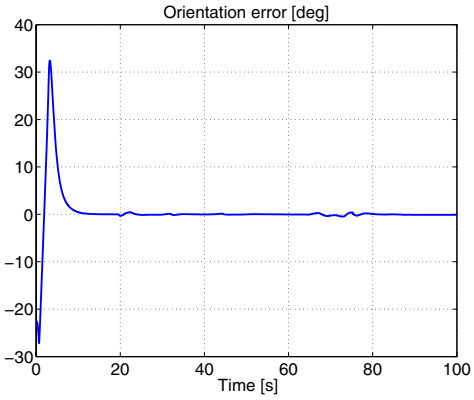

Fig. 10. The orientation error (θ_e)

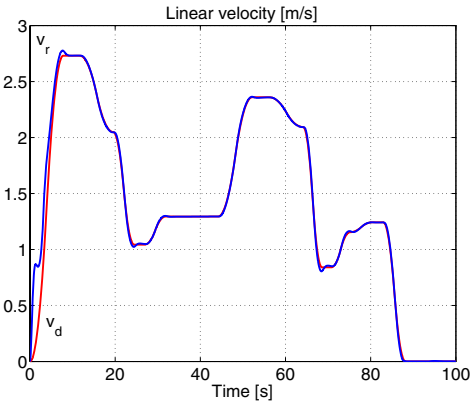

Fig. 12. The linear velocity $(v_d$ and $v_r)$

Fig. 8. We observe that all the errors (x_e, y_e, θ_e) converge to zero. The trajectory-tracking task must perform not only the planning of the curve (spatial dimension) but also the speed profile (temporal dimension).

Figures 13-15 show the results for path-following case without initial pose error. In the path-following task, the lateral error, y_e, is defined as the distance between the vehicle control point and the closest point along the vehicle desired trajectory, described by coordinates (x_d, y_d, θ_d). The desired velocity profiles, depicted in Fig. 2, were used in path-following simulations.

VII. CONCLUSION

This paper describes a strategy for trajectory-tracking and path-following control of car-like vehicles. A new design of sliding surface for control, together with a smooth velocity planner (imposing the comfort of human body), was proposed. The main advantages of using SMC include fast response, good transient and robustness with respect to system uncertainties and external disturbances.

.

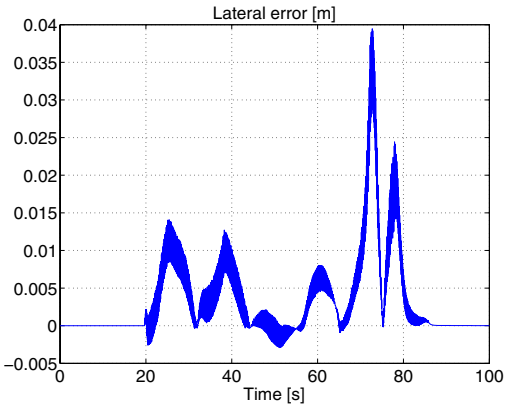

Fig. 13. The lateral error (y_e) for path-following

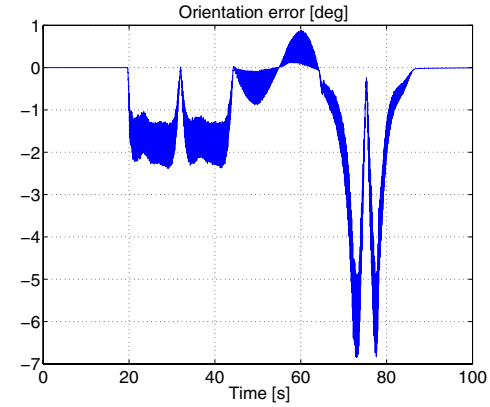

Fig. 14. The orientation error (θ_e) for path-following

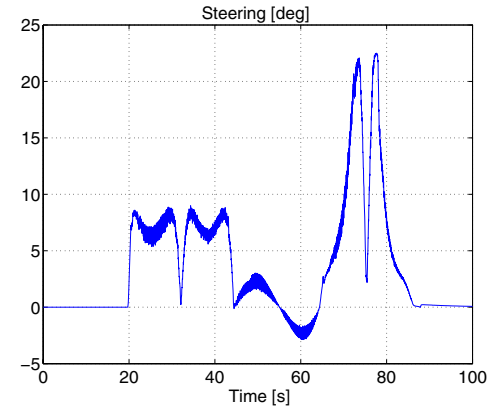

Fig. 15. The steering angle (ϕ_r) for path-following

REFERENCES

[1] M. Parent, G. Gallais, A. Alessandrini and T. Chanard, Cybercars: review of first projects, *Ninth Int. Conf. an Automated people Movers*, Singapore, 2003.

[2] Cybercars. *Cybernetic techologies for the car in the city*, [online], www.cybercars.org.

[3] U. Nunes and M. Parent, Special issue on robotics technologies for intelligent road vehicles, *Autonomous Robots*, Springer-Verlag, vol. 19 (12), 2005.

[4] F. Wang, N. Ma and H. Inooka, A driver assistant system for improvement of passenger ride comfort through modification of driving dehaviour, *Int. Conf. on Advanced Driver Assistance Systems*, vol. 483, 2001, pp.38-42.

[5] J. Forstberg, Human responses to motion environments in train experiment and simulator experiments, *PhD thesis*, Royal Institute of Tehnology - Stockholm, 2000.

[6] R.Fierro and F.L. Lewis, Control of a nonholonomic mobile robot: backstepping kinematics into dynamics, *Proceedings of the 34th Conference on Decision and Control*, New Orleans, LA, Dec. 1995, pp.3805-3810.

[7] G.F. Yuan, Tracking control of a mobile robot using neural dynamics based approaches, *Masters Abstracts International*, vol.39-05, Apr. 2001, pp.1437.

[8] K. D. Young, V. I. Utkin, and U. Ozguner, A control engineer's guide to sliding mode control, *IEEE Transactions on Control Systems Technology*, vol. 7, no. 3, pp. 328-342, 1999.

[9] Slotine J.J.E. and W.Li, *Applied Nonlinear Control*, Prentice-Hall Inter. Ed., 1991.

[10] ISO, Mechanical vibration and shock evaluation of human exposure to whole body vibration - part 1: General requirements, *ISO 2631-1*.

[11] C.G. Lo Bianco, A. Piazzi, and M. Romano, Velocity planning for autonomous vehicles, *IEEE Inteligent Vehicles Symposium*, Univ of Parma, Italy, June 14-17, 2004, pp 413-418.

[12] C.G. Lo Bianco, A. Piazzi and M. Romano, Smooth Motion Generation for Unicycle Mobile Robots Via Dynamic path Inversion, *IEEE Trans. on Robotics*, Vol. 20, No. 5, Oct. 2004, pp. 884-891.

[13] A. Piazzi and C. G. Lo Bianco, Quintic G2-splines for trajectory planning of autonomous vehicles, *IEEE Intelligent Vehicles Symposium*, Dearborn (MI), USA, Oct. 3-5, 2000, pp. 198-203.

[14] J-M. Yang and J-H. Kim, Sliding Mode Control for Trajectory Tracking og Nonholonomic Wheeled Mobile Robots, *IEEE Trans. on Robotics and Automation*, Vol. 15, No. 3, June 1999, pp. 578-587.